

DELIVERABLE REPORT



NEXUS

D3.3: Perovskite/Si tandem module demonstrator with >30% PCE

**Deliverable D3.3
OCTOBER-2025**

**PREPARED BY
CEA
COORDINATED BY
CEA**

Grant Agreement n°101075330

NEXUS is a 3-year research and innovation project funded by the European Commission through the Horizon Europe Research and Innovation Action (RIA) grant N°101075330, responding to the call for a “Sustainable, secure and competitive energy supply” (HORIZON-CL5-2021-D3-02).

NEXUS aims to accelerate Europe’s energy transition by developing perovskite-silicon tandem photovoltaic technology, via a new European paradigm: an eco-design approach, based on efficiency, cost, sustainability, circularity and social aspects and using abundant materials. NEXUS aims to develop stable, 2-terminal perovskite-silicon tandem solar cells and modules with high power conversion efficiencies, using sustainable, coherent and competitive European PV production, to create a viable economic pathway for the European commercialisation of this technology.

NEXUS is formed of a multi-disciplinary consortium: 13 partners from 10 countries; 6 industrial partners & 7 RTOs, covering the whole value chain of innovation from research centres to technology providers, end-users and market and policies.

Project info	101075330 – NEXUS – HORIZON-CL5-2021-D3-02-04
Deliverable Title	D3.3: PVS/Si tandem module demonstrator with 30% PCE
Lead Beneficiary	Commissariat à l’Énergie Atomique et aux Énergies Alternatives
Authors	P. Carroy, D. McMeekin
Approved by	H.J. Snaith
Dissemination level	Public
Due date	31/10/2025
Submission date	10/11/2025
Version	V1
Linked to WP - task	WP3 – 3.1 Module development



NEXUS

Project N°101075330.

NEXUS D3.3: Perovskite/Si tandem module demonstrator with >30% PCE

Legal notice

This document only reflects the authors' view, and the Union is not liable for any use that may be made of the information contained therein.

© This document is the property of the NEXUS Consortium. This document may not be copied, reproduced, or modified in whole or in part for any purpose without written permission from the NEXUS Consortium, which consists of the following participants:

NEXUS Consortium

Organization name	Short name	Country
COMMISSARIAT A L'ENERGIE ATOMIQUE ET AUX ENERGIES ALTERNATIVES	CEA	FR
ACCADEMIA EUROPEA DI BOLZANO	EURAC	IT
KARLSRUHER INSTITUT FUER TECHNOLOGIE	KIT	DE
RIJKSUNIVERSITEIT GRONINGEN	RUG	NL
SALD B.V	SALD	NL
UNIVERSITAT DE VALENCIA	UVEG	ES
3 SUN S.R.L.	3SUN	IT
ICARES CONSULTING	BI	BE
NORSUN AS	NORSUN	NO
THE CHANCELLOR, MASTERS AND SCHOLARS OF THE UNIVERSITY OF OXFORD	UOXF	UK
OXFORD PHOTOVOLTAICS LIMITED	OPV	UK
FACHHOCHSCHULE NORDWESTSCHWEIZ	FHNW	CH
ODTU GUNES ENERJISI UYGULAMA VE ARA STIRMA MERKEZI	GUNAM	TR



eurac
research



rijksuniversiteit
groningen



Fachhochschule
Nordwestschweiz



© Members of the NEXUS Consortium

Disclaimer

Funded by the European Union. Views and opinions expressed are however those of the author(s) only and do not necessarily reflect those of the European Union or CINEA. Neither the European Union nor the granting authority can be held responsible for them.

How to Cite

P. Carroy, D. McMeekin, H.J. Snaith (2025). Deliverable 3.3 Report: Perovskite/Si tandem module demonstrator with >30% PCE. in Project NEXUS: Next Generation of Sustainable Perovskite-Silicon Tandem Cells (No. 101075330). European Union. PUBLIC.

Table of Content

Table of Content.....	4
List of Tables.....	5
List of Figures.....	5
Abbreviations and acronyms list.....	6
1. Executive Summary.....	7
1.1. Description of the deliverable content and purpose.....	7
1.2. Relation with other activities in the project.....	7
2. Single-cell laminates.....	8
2.1. Single-cell devices made at CEA.....	8
2.2. Single-cell laminates made by UOXF.....	12
3. Perovskite-silicon tandem modules.....	16
4. Conclusions.....	17
References.....	18

List of Tables

Table 1: BoM used on the first NEXUS tandem modules	8
Table 2: Average, median and standard deviation of the IV parameters measured on the PST devices encapsulated at CEA, discarding the outliers depicted in the text.	10
Table 3: Average, median and standard deviation of the IV parameters measured on the PST devices received by CEA for encapsulation, limiting the dataset to the PST cells that were light-soaked prior to measurement at CEA.....	11
Table 4: Average CtL ratio of IV parameters calculated for PST devices encapsulated at CEA having the same “light-soaking status” before and after lamination.	11
Table 3: JV parameters measured on the PST devices before and after lamination using the in-house oxford lamination system.....	15
Table 5: IV parameters extracted from reverse IV measurements of the two 4-cell mini-module demonstrators made by NEXUS consortium.....	17

List of Figures

Figure 1: Example of a tandem sample featuring two independently-connected cells, a smaller one of 0.25 cm ² active area and a larger one of 1 cm ² active area.	8
Figure 2: Performances of the PST cells measured “as-fabricated” at the “top cell” partner (Initial @partner) and at CEA, before and after lamination PCE (top left), FF (top right), V _{OC} (bottom left) and J _{SC} (bottom right) extracted from reverse IV measurements under STC (n = 57). The notches correspond to a 95% confidence interval around the median.....	9
Figure 3: Examples of PST cells from the batch that suffered for which numerous issues with ribbon gluing occurred.....	10
Figure 4: UOXF in-house designed and constructed lamination system	12
Figure 5: An exploded view of a laminated solar cell stack	13
Figure 6: A picture of a laminated perovskite/Si tandem solar cell showing delamination of the polyolefin film, with the darker circle in the middle being the appropriately laminated region, and the lighter periphery being delaminated.	14
Figure 7: A picture of a successfully laminated perovskite/Si tandem solar cell showing no signs of delamination	14
Figure 8: Current-voltage sweep of a perovskite/c-Si solar cells a) before encapsulation and b) after lamination	15
Figure 10: Pictures of the two mini-module demonstrators each made with four cells interconnected in series: on the left, first demonstrator, as presented in the report associated to milestone 6 and on the right, second demonstrator made at the end of the project.....	16

Abbreviations and acronyms list

Abbreviation	Meaning	Abbreviation	Meaning
BoM	Bill of Material	Jsc	short-circuit current density
CAD	computer aided design	PCB	printed circuit board
CtL	cell-to-laminate	PCE	power conversion efficiency
CtM	cell-to-module	POE	polyolefin elastomer
FF	fill factor	PST	perovskite/silicon tandem
ITO	indium tin oxide	PVSK	perovskite
IV	current-voltage	STC	standard testing conditions
IZO	indium zinc oxide	Voc	open-circuit voltage

1. Executive Summary

1.1. Description of the deliverable content and purpose

Overview: This deliverable relates to the creation of a perovskite-on-silicon tandem module demonstrator. Herein, we summarise the processes which were developed to enable this and that were described in detail in D3.2, namely cell lamination material selection and lamination process and cell interconnection development. We detail the results obtained with multiple single-cell laminates and those achieved recently with the creation of two 4-cell modules, which achieved cell-to-module losses of less than 10%. However, the overall efficiency of the best 4-cell module was considerably lower than the target, at only 20%. This was largely due to the lower than targeted starting efficiency of the individual cells. In addition, we had originally planned to integrate 10*10 cm² cells into the module. Due to challenges in producing large area cells described in D2.2, we employed cells with a 4.4 cm² active area, giving our 4-cell module an active area of 13.6 cm². The best efficiency obtained with a single-cell laminate was 24.1% on a device with 1 cm² active area.

Analysis: We experienced many challenges with this deliverable. Firstly, work up of the cell lamination process was hampered by the low availability of tandem cells early on in the project. An early failure of laminates was observed due to the delamination of the ribbon. However, we advanced the lamination process with “single-cell” laminates, which then enabled distribution for outdoor stability work within the project and we successfully worked up lamination in two sites, CEA and UOXF. Due to the challenges with larger area processing on complete M2 wafers, we created an intermediate cell design, which is described in D2.2, comprising a larger single cell centred within a 3*3 cm² cut wafer. This enabled the fabrication and supply of a number of the larger cells which were successfully worked up into 4-cell minimodules.

Call to action: The overall efficiency of the modules is hampered by the low efficiency of the initial cells. We did also observe issue with shipping cells between partners. Hence, the pathway to enable higher efficiency modules is to fabricate higher efficiency large area cells, and either fabricate the modules at site of cell fabrication, or develop more robust cells and shipping protocols, to enable cells to be successfully shipped between partners.

1.2. Relation with other activities in the project

This Deliverable was directly influenced by WP2, and specifically the content of D2.2 *Full PVSK/Si cell demonstrator with sustainable design and scalable processes, PCE >33%, for active area > 0.5 cm² and PCE > 31%, for 100 cm² active area which is the fabrication and delivery of perovskite-on-silicon tandem cells.*

These deliverable influences work in WP4 related to outdoor stability assessments, and specifically the work reported in D4.2 *Full assessment of degradation mechanisms in NEXUS high performing PVSK/Si modules (> 12 months).*

2. Single-cell laminates

One of the most critical deviation the description of action mentioned in the mid-term report, was the delay in the fabrication of modules/encapsulated devices due to the unanticipated long learning process at the cell level that was necessary to obtain functional tandem solar cells in the consortium. As a large number of samples were required to address the various activities involving the encapsulation of tandem devices (including, of course, the development itself of module-related processes such as encapsulation and interconnection, but also, outdoor monitoring at four sites, including both electrical measurement and assessment of the environmental impact of lead, as well as indoor reliability testing), most of the 'modules' fabricated during the project actually are single-cell encapsulated devices. It would have been impossible to address all topics using interconnected mini-modules made of four cells or more. Nevertheless, these single-cell laminates were fabricated using the same materials and processes as those used for a mini-module, in terms of both encapsulation and cell connection.

2.1. Single-cell devices made at CEA

The development of the module Bill of Material (BoM) used at CEA was described in deliverable 3.2 *BOM definition for eco-designed PVSK/Si tandem modules passing IEC tests*. Its ability to protect the perovskite/silicon tandem (PST) cells against harsh environment like damp-heat (85°C, 85% relative humidity) and to withstand extreme temperature changes (-40°C to 85°C) was demonstrated in the report associated to milestone 6 *Interim tandem module milestone: Encapsulated proof of principle 4-cell PVSK/Si module, cell-to-module loss < 10%, passing IEC stability tests*. As a reminder, the composition of the BoM used at CEA is summarised in Table 1.

Module BoM	
Front cover	100 x 100 x 3mm glass
Encapsulant	Thermoplastic Polyolefin
Rear cover	100 x 100 x 3mm glass
Edge sealant	Polyisobutyl 10mm x 650µm
ECA	Acrylate
Ribbons	800 x 200µm

Table 1: BoM used on the first NEXUS tandem modules

All encapsulated tandem solar cells were fabricated by the consortium on silicon heterojunction (SHJ) bottom cells made by CEA on industrial Czochralski (Cz) wafers with vacuum- or hybrid-processed perovskite top cell made by UOXF, KIT or UVEG. In total, about 40 samples were successfully encapsulated at CEA, without visible breakage (glass, ribbon, cell). Among them, 17 featured two independently-connected cells, as shown in the example of Figure 1, allowing for more data generation.

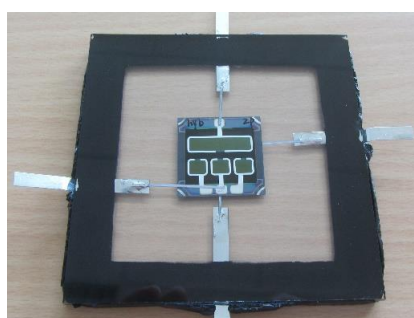


Figure 1: Example of a tandem sample featuring two independently-connected cells, a smaller one of 0.25 cm² active area and a larger one of 1 cm² active area.

The performances of the PST cells are plotted in Figure 2 that displays the power conversion efficiency (PCE), fill factor (FF), open-circuit voltage (V_{oc}) and short-circuit current density (J_{sc}) of the cells extracted from reverse current-voltage (IV) sweeps measured under standard testing conditions (STC). The IV measurements were performed by the partner who fabricated the perovskite top cell (“Initial @partner”) and at CEA upon receipt (i.e., before lamination) and after lamination. Table 2 displays the average, median and standard deviation of the measured parameters. Four outliers were removed from the original dataset of Figure 2 to calculate the values represented in Table 2. These are the four datapoints that can be seen well below the boxplots of the PCE and J_{sc} measured after lamination in Figure 2. These four data points correspond to four devices of the same batch of PST cells, for which there were many issues with the silver contacts of the cells that tended to delaminate when the gluing the metallic ribbons onto them (see Figure 3). Although the gluing process seemed successful for these four devices, we suspect that the silver contact may have delaminated subsequently, for example during lamination. It is very difficult to observe possible delamination of the silver contact in the laminated device, since all layers are “pressed” together. However, the very low carrier collection seems to indicate an absence of electrical contact between the cell and the ribbon. Therefore, we suspected that these visually flawless devices were affected by the same issue as their sister devices and they were thus excluded from the calculations in Table 2.

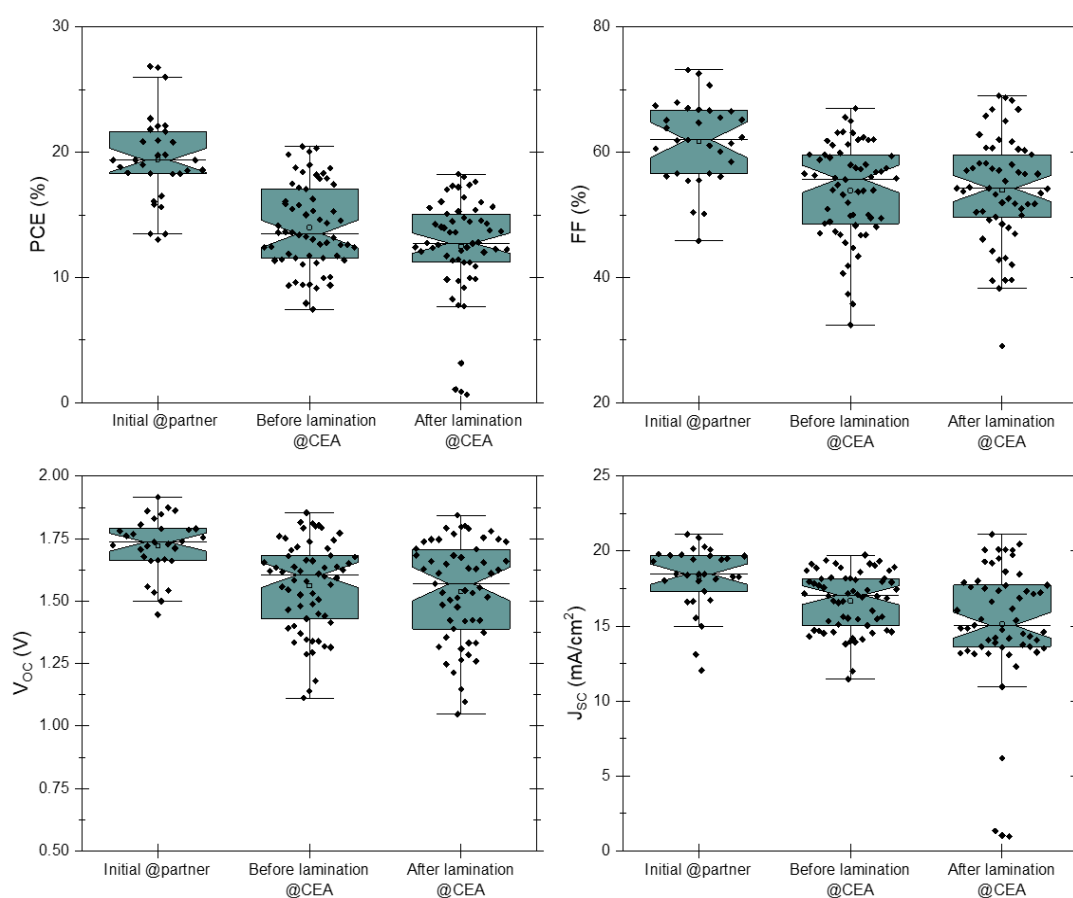
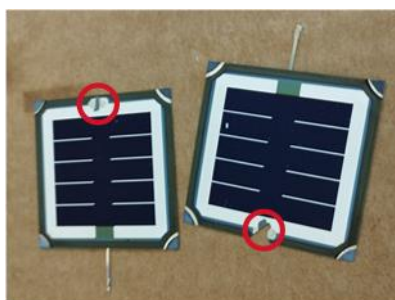


Figure 2: Performances of the PST cells measured “as-fabricated” at the “top cell” partner (Initial @partner) and at CEA, before and after lamination PCE (top left), FF (top right), V_{oc} (bottom left) and J_{sc} (bottom right) extracted from reverse IV measurements under STC ($n = 57$). The notches correspond to a 95% confidence interval around the median.

**Table 2: Average, median and standard deviation of the IV parameters measured on the PST devices encapsulated at CEA, discarding the outliers depicted in the text.**

n = 53		J _{sc} mA/cm ²	V _{oc} V	FF %	PCE %	J _{sc}	V _{oc}	FF	PCE
						Relative changes with respect to previous measurement step			
Initial @partner	Average	18.7	1.72	61.9	19.9	N.A.	N.A.	N.A.	N.A.
	Median	18.5	1.73	62.4	19.4	N.A.	N.A.	N.A.	N.A.
	Standard deviation	1.5	0.12	6.6	3.1	N.A.	N.A.	N.A.	N.A.
Before lamination @CEA	Average	16.9	1.55	53.9	14.1	-9.5%	-9.8%	-13.0%	-29.0%
	Median	17.2	1.59	55.8	13.6	-7.0%	-8.1%	-10.7%	-29.9%
	Standard deviation	1.8	0.18	7.8	3.4				
After lamination @CEA	Average	16.1	1.54	54.6	13.3	-4.8%	-0.9%	1.3%	-5.4%
	Median	15.5	1.57	54.2	13.6	-9.9%	-1.2%	-2.7%	0.1%
	Standard deviation	2.6	0.20	7.7	2.6				

**Figure 3: Examples of PST cells from the batch that suffered for which numerous issues with ribbon gluing occurred.**

The data from Figure 2 and Table 2 indicate a significant drop in all IV parameters when the PST cells are measured upon receipt at CEA, compared to the initial measurement after their fabrication by the top cell partner. The average PCE measured at CEA is approximately 6 points lower than the initial average PCE (corresponding to a 30% relative degradation), due to an average V_{oc} that is 170 mV lower, an average J_{sc} around 1.8 mA/cm² lower and an average FF around 8 points lower. Unfortunately, the reason for this difference is still unclear.

To investigate this, some cells were sent back to the partner who had fabricated them for re-measurement, to rule out measurement issues or cell degradation. It was observed that most of the performance loss could be recovered after light-soaking the cells at 1 sun during several minutes, thereby revealing a metastability behaviour of the devices, that tend to degrade when stored in the dark and then recover when exposed to light, a behaviour which has already been observed in perovskite-based devices [1], [2], [3] and that we also observe in the outdoor performance of NEXUS' devices¹. In some samples the recovery, although significant, was not entirely complete, which could indicate a certain degree of irreversible degradation of these samples or an insufficient light exposure to ensure full recovery. A light-soaking protocol prior to measurement, consisting of a 15 minutes

¹ See deliverable 4.2 *Full assessment of degradation mechanisms in NEXUS high performing PVSK/Si modules (> 12 months)*

exposure at 1 sun illumination, was then implemented at CEA. Table 3 displays the IV parameters of a dataset limited to cells that were light-soaked prior to measurement when received by CEA. We observe that the difference between the initial measurement by the “top cell” partner and CEA’s measurement is reduced compared to Table 2. However, the average PCE measure at CEA is still significantly lower, by 3.5 points, suggesting a probable irreversible partial degradation of the samples. Unfortunately, due to the limited quantity of samples available to support activities requiring encapsulated cells, as well as the already existing delay in implementing these activities, we were unable to allocate time or samples to further investigate this suspected degradation. We tried to adapt shipping protocols, ensuring that the cells were sealed in a neutral atmosphere before being shipped. However, there was still a performance gap observed before and after shipment.

Table 3: Average, median and standard deviation of the IV parameters measured on the PST devices received by CEA for encapsulation, limiting the dataset to the PST cells that were light-soaked prior to measurement at CEA.

n = 30		J _{sc} mA/cm ²	V _{oc} V	FF %	PCE %
Initial @partner	Average	18.7	1.68	59.5	18.6
	Median	19.4	1.72	61.0	19.0
	Standard deviation	2.1	0.10	7.0	3.1
Before lamination @CEA	Average	17.2	1.56	55.8	15.1
	Median	17.9	1.60	56.3	14.6
	Standard deviation	2.0	0.15	5.9	3.0

The metastability of the samples and their potential degradation during transportation (or simply their aging with time) makes it difficult to assess the impact of the lamination process on cell performance with precision. Nevertheless, we can make a rough evaluation by examining the statistics in Figure 2 and Table 2. Figure 2 reveals a similar distribution of the IV parameters before and after lamination. The box notches indicate that there is no statistical difference in the PCE, FF and V_{oc} values measured before and after lamination. However, the J_{sc} values appear to be statistically lower after lamination than before: Table 2 shows a reduction of 4.8% and 9.9% in the average and median J_{sc}, respectively. The lower current delivered by the encapsulated devices can be partially explained by the fact that many of the samples that were received for encapsulation had an antireflective coating to enhance the current at cell level. However, this leads, on the contrary, to non-optimal optical coupling after glass encapsulation (as can be seen, for example, from the greenish colour observed on the cell areas in Figure 1).

Table 4: Average CtL ratio of IV parameters calculated for PST devices encapsulated at CEA having the same “light-soaking status” before and after lamination.

n = 36	J _{sc}	V _{oc}	FF	PCE
Average CtL ratio	93.8%	96.8%	101.4%	92.1%

To obtain a more precise quantification of the evolution of cell performance upon lamination, we calculated the ratio between the PCE, FF, V_{oc} and J_{sc} values after lamination versus before lamination for each encapsulated device. This is analogous to the Cell-to-Module (CtM) power ratio, which is commonly used to quantify the impact of integrating solar cells into modules by dividing the module power by the sum of the power of the individual cells used to make the module. In the present case, we could refer to it as the “Cell-to-Laminate” (CtL) ratio, given that we are only considering single-cell devices. For the calculation of the IV parameters CtL ratio of each encapsulated cell, we selected devices that had the same “light-soaking status” before and after lamination; that is to say, they were

either light-soaked before AND after lamination, or not at all. It could indeed happen that, due to lack of time, some cells were not light-soaked before their pre-lamination measurement, but were light-soaked before their post-lamination measurement, which could have introduced a significant bias in the CtL calculation. Table 4 shows the average CtL ratio for the different IV parameters calculated for these devices. The average CtL power ratio is 92.1%, indicating a CtL loss in power of 7.9%. This is better than the 10% loss specified as the target to achieve Milestone 6. This CtL power loss is due to both a V_{oc} and J_{sc} loss of 3.2 and 6.2% respectively.

Overall, the performance level of the encapsulated cells is low, with a PCE of about 15.1% in average. The maximum PCE measured after encapsulation is 18.3% on these single-cell devices, well below the module target of 30%. This is mainly due to the low performance level of the cells as received by CEA. Indeed, the statistics suggest that the encapsulation process itself does not cause significant damage to the cells and should not impede the achievement of high efficiencies at the module level with high performing cells.

2.2. Single-cell laminates made by UOXF

At UOXF, we designed and built a lamination system. This home-built lamination system allowed us to laminate single-junction perovskite solar cells on Indium-Tin-Oxide (ITO) glass and perovskite/c-Si solar tandem solar cells on CEA-processed wafer. Both of these laminates were 30x30 mm in size. Our in-house design allowed us to laminate the solar cells in the inert atmosphere using a nitrogen (N_2) filled glovebox. In Figure 4, we present the computer aided design (CAD) drawing of the hardware used to laminate the perovskite/Si tandem that were aged in outdoor conditions at EURAC (Bolzano) and UVEG (Valencia). Although it was not initially planned for UOXF to develop a lamination process in the framework of the project, this alternative emerged as a particularly interesting option. Indeed, it enabled the encapsulation of tandem cells manufactured by UOXF itself, thereby avoiding the need to ship some samples to an external partner and the associated risk of degradation during transport.

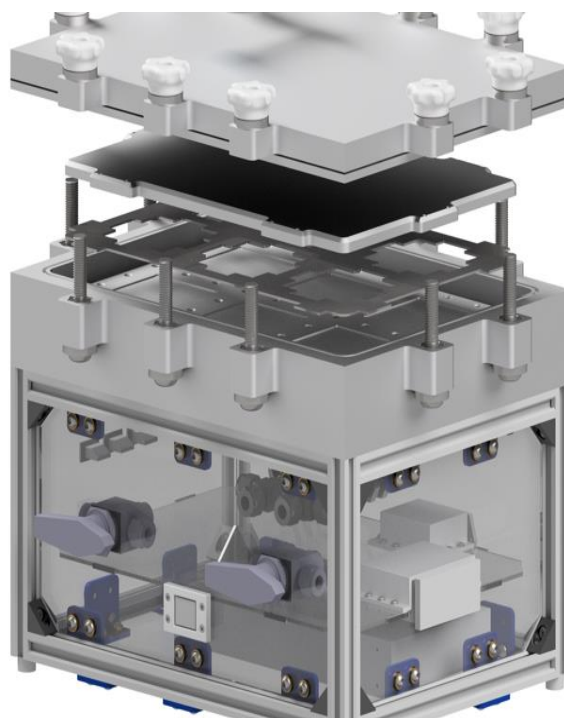


Figure 4: UOXF in-house designed and constructed lamination system

The lamination system consists of two chambers separated with a membrane. Initially, both chambers are evacuated in order to remove any gas that might be trapped within the laminate. The laminate is then heated to 130° C soften the encapsulant materials (Kömmerring Helioseal butyl rubber, Mistui TR04BA-50T POE encapsulant). Once the laminate is appropriately heated, the upper chamber is refilled to atmospheric pressure and the membrane is pressed down onto a PTFE plate to distribute the load of the membrane and prevent uneven pressure due to inconsistent stretching at the edge of the membrane. This plate is pressed down onto a spacer layer of appropriate thickness to limit the total compression of the laminate. The system is left in this state for a further 5 minutes to promote adhesion between the polyolefin elastomers (POE) encapsulant and the device layer before the lower chamber is vented and the laminates removed and allowed to cool slowly to prevent damage from thermal shock.

In Figure 5, we show an exploded view of a laminated solar cell stack. These laminates incorporate a Printed Circuit Board (PCB) into their construction to transfer the electrical connections from the device from the inside of the laminate to an external measurement system. The solar cell is inserted inside the middle of the PCB, where silver tape with electrically conductive adhesive connects the electrodes from the solar cell to the PCB. The solar cell is then sandwiched in-between two POE films, which is then sandwich between two glass sheets. This stack is then vacuum laminated in an N₂ atmosphere using the home-built lamination system.

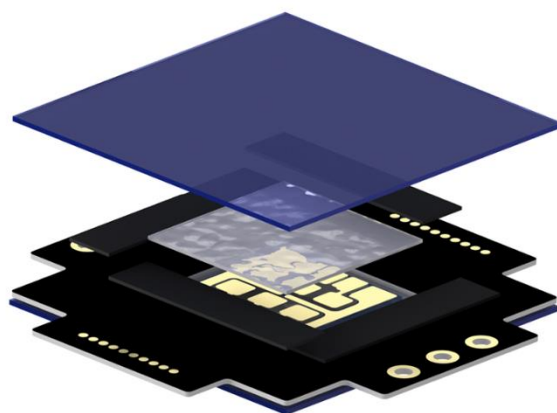


Figure 5: An exploded view of a laminated solar cell stack

Initial tests exhibited delamination of the POE encapsulant from the PST device, resulting in optical defects within the laminate. Figure 6 shows the delamination of the POE and the glass that occurs over time if the lamination process is not ideal.

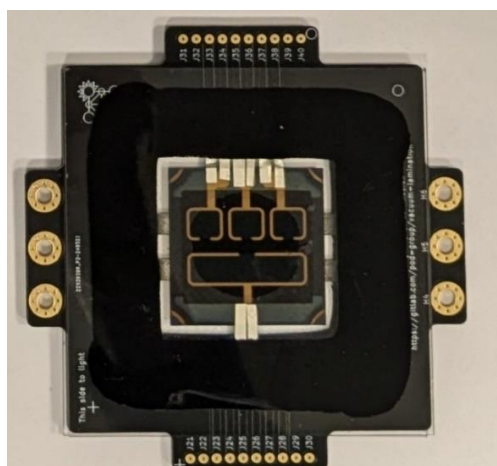


Figure 6: A picture of a laminated perovskite/Si tandem solar cell showing delamination of the polyolefin film, with the darker circle in the middle being the appropriately laminated region, and the lighter periphery being delaminated.

To combat this, the stack was altered to include additional POE encapsulant and the process was altered to stay at temperature for longer to promote better adhesion. Subsequent laminations following these changes did not exhibit these defects (shown in Figure 7).

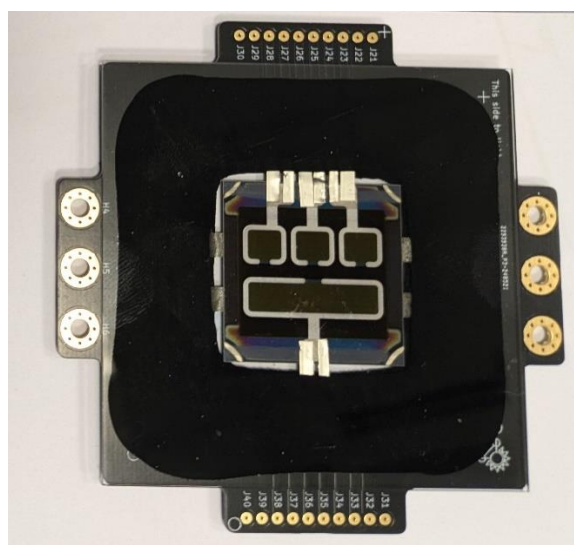


Figure 7: A picture of a successfully laminated perovskite/Si tandem solar cell showing no signs of delamination

In Figure 8, we show the JV characteristics of the champion laminated perovskite/nano-textured silicon tandem. Due to the thick glass laminate, there exists a large gap between the illumination mask and the device, which causes the PCE measurement to be inaccurate since the gap causes light to be shined outside of the electrode area. This is due to the solar simulator light being not perfectly collimated. Therefore, we measured the JV characteristics of an unmasked area device and applied a ratio of 0.847 to the current density and PCE, which is the J_{SC} ratio between a mask and unmasked cell. This ratio was obtained by measuring the current-density of the device using an illumination mask that is much smaller (0.0919 cm^2) than the electrode area in order to obtain an accurate measurement of the J_{SC} , which should account for any divergent sunlight.

Prior to the lamination, the PST measured 25.6% PCE with an V_{oc} of 1.91V, a FF of 74.8% and a J_{sc} of 17.9 mA/cm², post lamination we measured an unmasked PCE of 28.41% (assuming the same area) with an V_{oc} of 1.86V, a FF of 65.0% and a J_{sc} of 23.5 mA/cm². Therefore, the corrected parameter values of the laminated perovskite/c-Si tandem solar cell measured 24.1% PCE with an V_{oc} of 1.86V, a FF of 65.0% and a J_{sc} of 19.9 mA/cm².

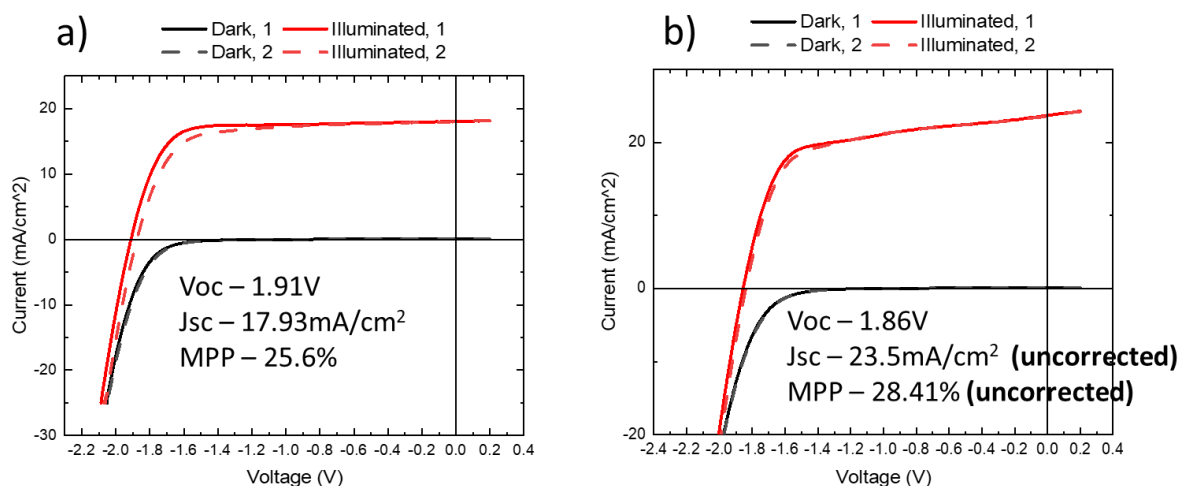


Figure 8: Current-voltage sweep of a perovskite/c-Si solar cells a) before encapsulation and b) after lamination

Table 5: JV parameters measured on the PST devices before and after lamination using the in-house oxford lamination system.

Champion laminated Device	J_{sc} mA/cm ²	V_{oc} V	FF %	PCE %
Before Lamination	17.9	1.91	74.8	25.6
After Lamination (uncorrected)	23.5	1.86	65.0	28.41
After Lamination (Corrected)	19.9	1.86	65.0	24.1

We attribute the J_{sc} gain to an improved index of refraction matching between the Indium-Zinc-Oxide (IZO)/polyolefin film/glass/air versus the IZO/air interface that is initially measured for un-laminated perovskite/c-Si tandem solar cells. However, we do observe the appearance of a slight shunt in the JV characteristics of the laminated tandem device, causing a lower FF in the laminated device. Overall, the PCE of the device was lowered by 1.5% absolute, corresponding to a CtL loss of 5.9%.

3. Perovskite-silicon tandem modules

The fabrication of a 4-cell mini-module demonstrator was an important milestone in the project and the results obtained with the first demonstrator made in the project (Figure 9) were already presented in the report associated to milestone 6. The fabrication of an actual two-terminal PST module, i.e., made with several series interconnected monolithic PST cells, is an important result, not only for the project, but also for the PST research community. Indeed, apart from press releases from recognised players in the field^{2,3}, there seem to be only one scientific article that describes the interconnection of several monolithic PST cells into a two-terminal module, in which the teams from Fraunhofer ISE and Oxford PV showcase commercial-size modules made with 120 M6 half cells [4].

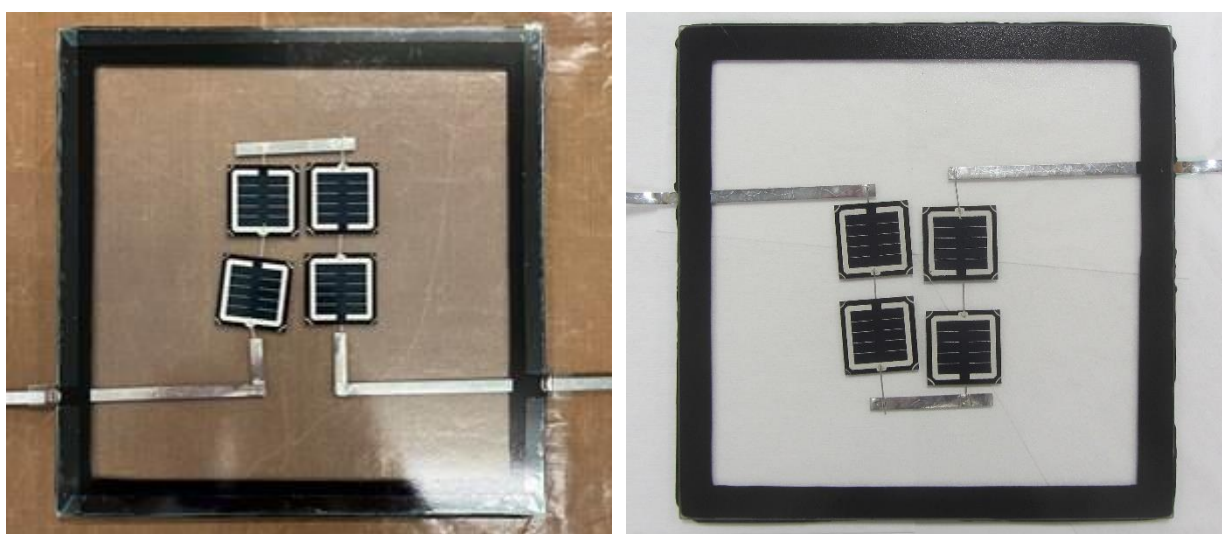


Figure 9: Pictures of the two mini-module demonstrators each made with four cells interconnected in series: on the left, first demonstrator, as presented in the report associated to milestone 6 and on the right, second demonstrator made at the end of the project.

Table 6 summarizes the results obtained with the first demonstrator and present new results obtained on a second demonstrator that was recently manufactured. This second module was made with PST cells very similar to those used in the first module: four 4.62-cm² active area PST cells made by UOXF with a sequentially-evaporated perovskite top cell on a silicon heterojunction bottom cell made by CEA on nanotextured Cz silicon. The module BoM remains the same as presented in milestone 6 and summarized in section 2.1. Table 6 shows that the two modules actually have higher efficiencies than all the single-cell devices of section 2.1. This is mainly because they were made towards the end of the project, on cells that had higher initial efficiencies. The first module reaches 18.9% PCE, corresponding to a power of 350 mW, while the second module shows an improved PCE of 20.1%, corresponding to a power of 372 mW. These two modules have a fairly satisfactory V_{OC} of about to 7 V, corresponding to a V_{OC} close to 1.8V per cell. The J_{SC} of the second module has improved compared to the first one and is now close to 19.5 mA/cm², which is also a fairly good value. The FF remains low, therefore strongly limiting the overall efficiency.

²<https://www.trinasolar.com/eu-en/resources/newsroom/eutrinasolar-develops-worlds-first-800w-tandem-module-ushering-new-era>

³<https://www.oxfordpv.com/press-releases/oxford-pv-solar-sustainability-initiative>

**Table 6: IV parameters extracted from reverse IV measurements of the two 4-cell mini-module demonstrators made by NEXUS consortium**

	J_{sc} mA/cm ²	V_{oc} V	$V_{oc}/cell$ V	FF %	P_{mpp} mW	PCE %
Module 1 (July 2025)	18.4	6.98	1.75	59.1	350	18.9
Module 2 (October 2025)	19.5	7.06	1.77	58.5	372	20.1

4. Conclusions

This report summarises the results obtained using PST cells encapsulated via an industrial process involving glass/glass lamination with a commercial encapsulant foil. The efficiencies obtained with these devices unfortunately lie well below the 30% target, with 20.1% obtained on a 4-cell mini-module and 24.1% on a single-cell encapsulated device. Achieving the 30% would have required cells with much higher initial efficiency (beyond 30%). Unfortunately, this is a number we also did not achieve in this project at the cell level, as described in deliverable 2.2. However, the data rather reassuringly indicates that the impact of the module manufacturing process on cell performance is limited, as the loss of performance after lamination remains less than 10% relative loss, which was the target aimed for in NEXUS. This is true for both lamination processes developed at CEA and UOXF. Nevertheless, it cannot be said with certainty that this finding is valid for higher-efficiency cells or cells that are less degraded prior to module assembly. Still, the results obtained on cells laminated at UOXF are reassuring in this respect: the cells, with higher initial efficiency and little or no degradation due to the absence of transport and reduced waiting time prior to encapsulation, also exhibited limited CtL losses.

Beyond the obvious need to develop high-efficiency solar cells, particularly on large surface areas, in order to obtain high-efficiency modules, this report raises the question of the possible impact of having a non-integrated value chain for the manufacture of PST modules, in particular the decoupling of module assembly from cell manufacturing. It highlights the importance of addressing the issue storing cells awaiting encapsulation in a way that ensures their stability and of developing shipping protocols that ensure this stability during transportation to a module manufacturer.



References

- [1] M. Khenkin *et al.*, « Light cycling as a key to understanding the outdoor behaviour of perovskite solar cells », *Energy Environ. Sci.*, vol. 17, n° 2, p. 602-610, janv. 2024, doi: 10.1039/D3EE03508E.
- [2] M. Remec *et al.*, « From Sunrise to Sunset: Unraveling Metastability in Perovskite Solar Cells by Coupled Outdoor Testing and Energy Yield Modelling », *Advanced Energy Materials*, vol. 14, n° 29, p. 2304452, 2024, doi: 10.1002/aenm.202304452.
- [3] M. Remec *et al.*, « Seasonality in Perovskite Solar Cells: Insights from 4 Years of Outdoor Data », *Advanced Energy Materials*, vol. 15, n° 35, p. 2501906, 2025, doi: 10.1002/aenm.202501906.
- [4] A. De Rose *et al.*, « Low-temperature metallization & interconnection for silicon heterojunction and perovskite silicon tandem solar cells », *Solar Energy Materials and Solar Cells*, vol. 261, p. 112515, oct. 2023, doi: 10.1016/j.solmat.2023.112515.